

Monitoring the sandstorm during spring season 2002 and desertification in northern China using SSM/I data and Getis statistics*

JIN Yaqui** and YAN Fenghua

(Center for Wave Scattering and Remote Sensing, School of Information Science & Engineering, Fudan University, Shanghai 200433, China)

Received August 22, 2002; revised December 12, 2002

Abstract A massive sandstorm enveloped most part of northern China during the spring season 2002. Monitoring the evolution of sandstorm and desertification has become one of the most serious problems for China's environment. Since 1989, one of the most advanced and operational passive microwave sensors is the DMSP SSM/I (special sensor microwave imager) operated at seven channels (19, 37, 85 GHz with the vertical and horizontal polarization and 22 GHz with vertical polarization only). In this paper, the sandstorm and desertification indexes, *SDI* and *DI*, are derived from the radiative transfer equation, and are employed with multi-channel measurements of the DMSP SSM/I for monitoring the sandstorm and desertification in northern China. Some SSM/I data in 1997 and 2001 are employed. The algorithm of Getis statistics is developed to categorize the spatial correlation and its evolution these days. It is demonstrated that the SSM/I indexes, *SDI* and *DI*, and its Getis statistics are well applicable for monitoring the sandstorm and desertification.

Keywords: microwave SSM/I, *SDI* and *DI* indexes, sandstorm, desertification, Getis statistics.

In recent years, serious sandstorms on different scales have been taking place in northern China, especially during March and April each year. A massive sandstorm enveloped most part of northern China on 19~20 March 2002, reported as the most significant one since the 1990s, and in some regions strong sandstorm was also observed^[1]. To monitor sandstorm and its temporal and spatial variations has become a critical issue for environment surveillance and protection in China. Desertification in northern China has also turned into a serious problem that keeps an annual increase, reaching 9.4% of the total Chinese land area^[2]. As an origin of sandstorms, Badain Jaran Desert and Tengger Desert tend to merge and expand. As a result, vegetation canopy in the adjacent region is diminishing, and even more seriously, the whole region becomes gradually desertified. For example, the tree canopy around Badain Jaran Desert has lost an area of nearly 2000 km² in the past 40 years. Additionally, owing to grassland degeneration and windy weather, the local desert area is constantly expanding and the extent of desertification becomes more serious.

The Defense Meteorological Satellite Program

(DMSP) Special Sensor Microwave/Imager (SSM/I) currently in operation since 1989 has 7 channels (19, 37, 85 GHz with dual polarization and 22 GHz with the vertical polarization only). The local time of descending (DS) and ascending (AS) flights of the satellite F13 is about 6 am and 6 pm, respectively, whereas the DS and AS time for F14 and F15 is about 09:30 am and 09:30 pm respectively. The spatial resolutions are correspondingly 15 km (85 GHz), 30 km (37 GHz) and 50 km (19 GHz). Satellite-borne microwave radiometer has become one of the most important tools for monitoring terrain surface because of its ability of all weather operation to penetrate through precipitation and continuous service for many years. Observation of DMSP SSM/I has been applied to invert physical, hydrological, biological and other scientific information from atmosphere, sea surface and land covers. However, how to monitor sandstorm and land desertification by use of satellite-borne microwave remote sensing has not been well studied.

In this paper, by using the vector radiative transfer (VRT) equation, sandstorm influence over the radiative properties is discussed. Employing multi-channel SSM/I data and VRT, we propose a sand-

* Supported by the National Key Basic Research Project (Grant No. 2001CB309401) and the National Natural Science Foundation of China (Grant No. 60171009)

** To whom correspondence should be addressed. E-mail: yqjin@fudan.ac.cn

storm index *SDI* to monitor the occurrence and evolution of sandstorm. Application of this index is demonstrated by using the SSM/I observation data of 19~21 March 2002 over Hunshandake Desert, Inner Mongolia and the adjacent region when a serious sandstorm happened. Polarization index, PI_{37} ^[3], namely desertification index *DI*, defined by the SSM/I data at 37 GHz channel, is employed for verification of spatial desertification, and two-year *DI* data of 1997 and 2001 over the Badain Jaran Desert and Tengger Desert are discussed. In order to evaluate the spatial correlation of regional radiative properties, the Getis spatial auto-correlation statistics is presented for *DI* index of the desert region to quantitatively describe desertification evolution in spatial scales.

1 Sandstorm index *SDI* defined by SSM/I data

The VRT equation for clear atmosphere is

$$T_{Bp} = (1 - r_p)e^{-\tau}T_s + (1 - e^{-\tau})(1 + r_p e^{-\tau})T_a, \quad (1)$$

$$p = v, h,$$

where r_p is p -polarized reflectivity of underlying surface, T_s the physical temperature of the land surface, T_a the averaged physical temperature of atmosphere, and τ the atmospheric opacity at this channel. For simplicity, suppose $T_s = T_a \equiv T_o$, whose possible difference is negligible in our analysis. We can have

$$T_{Bp} = (1 - r_p e^{-2\tau})T_o. \quad (2)$$

Because the sand particles are very small with the radius a about 0.15 mm unequally, under Rayleigh approximation ($ka \ll 1$ at low frequency, here k denotes the wave number), the scattering, absorption and extinction coefficients κ_s , κ_a , κ_e of the sand particles can be written as^[4]

$$\kappa_e = \kappa_s + \kappa_a = 2fk^4 a^3 \left| \frac{\epsilon_{sr} - 1}{\epsilon_{sr} + 2} \right|^2 + fk \frac{\epsilon_{sr}''}{\epsilon_{sr}'} \left| \frac{3}{\epsilon_{sr} + 2} \right|^2, \quad (3)$$

where $\epsilon_{rs} = \epsilon_{sr}' + i\epsilon_{sr}''$ is the relative dielectric constant of sand particles, f the particles' fraction volume per unit volume in the sandstorm layer.

According to the report of March 2002 by the surveillance network of the China State Environment Protection Administration (SPEA), we take the sandstorm parameters as follows: $a = 0.15$ mm, fractional volume $f = m/\rho = 5.5 \times 10^{-9}$, where total weight per unit cubage $m = 0.011$ g/m³ and the sand density $\rho = 2 \times 10^6$ g/m³ were measured. Assuming

the thickness of sandstorm layer be $d = 3$ km, and relative dielectric constant $\epsilon_{rs} = 5.0 + i0.25$ ^[5], the opacity of sandstorm layer is calculated as

$$\tau_s = \kappa_e d \sec \theta. \quad (4)$$

At the channel 85 GHz and SSM/I observation angle $\theta = 53^\circ$, it yields $\tau_{85} \approx 1 \times 10^{-3}$. It is known that the opacity of standard atmosphere at 85 GHz is about $\tau_{85} \approx 0.22$ or more^[4]. It can be seen that the sandstorm opacity would not be able to significantly affect whole atmospheric opacity. In other words, one cannot identify any significant changes of the opacity from microwave radiometers in satellite-borne remote sensing.

Sandstorm existence would affect radiative transfer from the underlying surface and most likely darken the difference between vertically and horizontally polarized reflectivities, as shown in Fig. 1. Polarization index $PI_{37} \equiv T_{B37v} - T_{B37h}$ has been used to characterize desert surface^[3], and scattering index $SI_{2285v} \equiv T_{B22v} - T_{B85v}$ has been used to describe the scattering difference between high (85 GHz) and low (22 GHz) SSM/I channels. It is noted that SI_{2285v} is a good indicator to detect rainfall. In our cases, there is no rainfall. Following Eq. (2), it is derived as

$$PI_{37} = (r_{37h} - r_{37v})e^{-2\tau_{37}}T_o, \quad (5)$$

$$SI_{2285} = (r_{85v}e^{-2\tau_{85}} - r_{22v}e^{-2\tau_{22}})T_o. \quad (6)$$

Both PI_{37} and SI_{2285} are the function of T_o and surface reflectivity r_p .

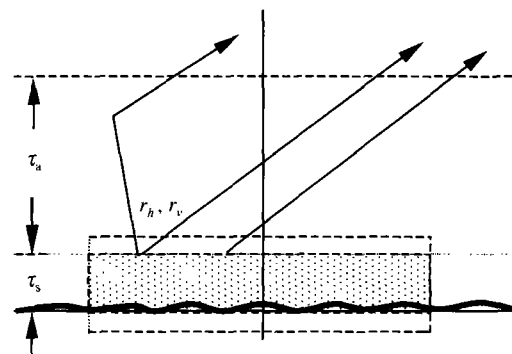


Fig. 1. Geometry of radiative transfer in sand stormy atmosphere.

We can simply assume that $r_{85v} \approx ar_{37v}$, $r_{22v} \approx \beta r_{37v}$ for dry surface, where α , β are actually very close to 1. To minimize the variation from T_o , we define the sandstorm index *SDI* as

$$SDI = \frac{SI_{2285}}{PI_{37}} = \frac{1}{(r_h/r_v) - 1} \cdot \frac{\alpha \cdot e^{-2\tau_{85}} - \beta \cdot e^{-2\tau_{22}}}{e^{-2\tau_{37}}}, \quad (7)$$

where r_h , r_v are the h , v -polarized reflectivities at 37 GHz, which take into account the sandstorm and underlying land surface indicated by the dashed line in Fig. 1. It always has $r_v < r_h$.

It can be seen that sandstorm makes r_v approach r_h , and increases SDI . The SDI from SSM/I measurements at 22 GHz, 37 GHz and 85 GHz is seen as a criterion for detecting sandstorm.

Region A in Fig. 2 underwent the sandstorm many times during 19 ~ 21 March 2002. Fig. 3 shows the averaged SDI from F13 DS data in region A during 19~25 March 2002. It can be seen that the rise of SDI on 20~21 March indicates the sandstorm occurrence.

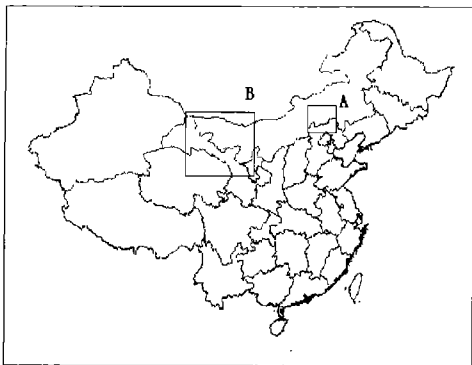


Fig. 2. Location of our study regions.

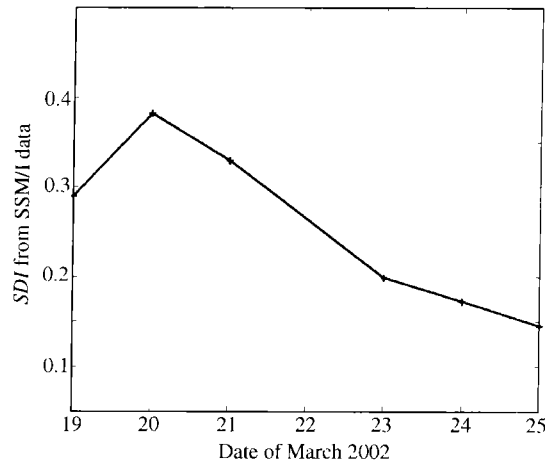


Fig. 3. Averaged SDI variations in region A before and after the sandstorm.

As the basis for comparison, Fig. 4(a) gives the averaged SDI of no sandstorm in region A during 23 ~ 25 March 2002. The brightness in Fig. 4(a) indicates high-value SDI , and dull blackness means low-value SDI .

Fig. 4(b) shows the SDI distribution in region A observed by DS-F13 on the morning of 21 March, 2002 when a sandstorm occurred. The difference between Fig. 4(b) and (a) is obtained as shown in Fig. 4(c), where the brightness is now due to the sandstorm occurrence of 21 March 2002.

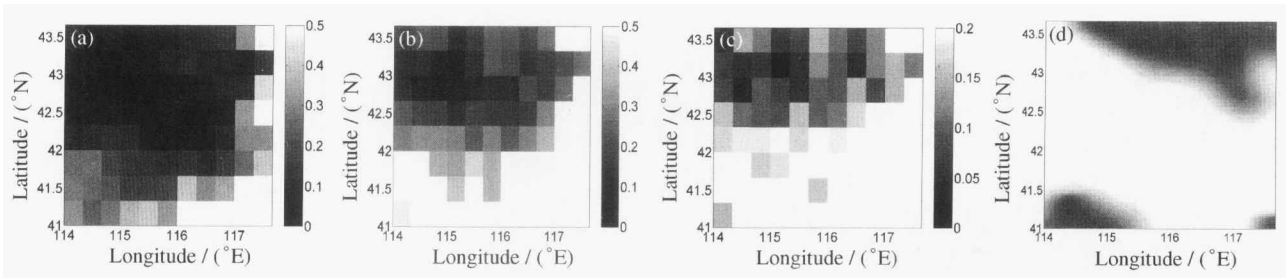


Fig. 4. SDI distribution. (a) SDI distribution without sandstorm, (b) SDI at 09:30 am on 21 March with a sandstorm, (c) SDI difference between (b) and (a) indicating the sand stormy region and (d) the sand stormy region at 12:00 on 21 March issued by China SSMC.

Fig. 4(d) was released to the Internet by China State Satellite Meteorology Center (SSMC) as a visualization of sandstorm occurrence at 12:00 on 21 March 2002 from observation of China Meteorological Satellite FY1-C. Fig. 4(c) is well validated by Fig. 4(d) if time difference between these two observations is taken into account.

2 Desert index DI for monitoring desertification

Desertification is characterized by canopy disap-

pearance, soil exposure and its conversion into sand. Dry sand surface drives a smaller difference between v , h -polarized reflectivities of land surface. We have defined the polarization index PI_{37} as a characteristic parameter for desert surface^[3]. We might as well name the desertification index

$$DI = PI_{37} = (r_h - r_v)e^{-2\tau T_o}. \quad (8)$$

Fig. 5(a) and (b) present the averaged DI distribution derived from SSM/I F13 over China's Badain Jaran Desert and Tengger Desert from March

to August in 1997 and 2001, respectively. Brightness in the figures depicts the desertification extent of two deserts.

It is noted that the regions with $DI > 20$ K in Fig. 5 (b) of 2001 have been expanded and the boundary between two deserts seems merged. Fig. 5 (c) shows the difference between Fig. 5(b) and (a)

to display the merging and expansion of two deserts. Fig. 5(d), especially, presents the DI variation at Yabulai Town (E103.0°, N39.6°), Inner Mongolia, from March to August 1997 and 2001. It demonstrates a significant increase of DI during the four years. It can also be seen that possible canopy during the summer season decreases DI .

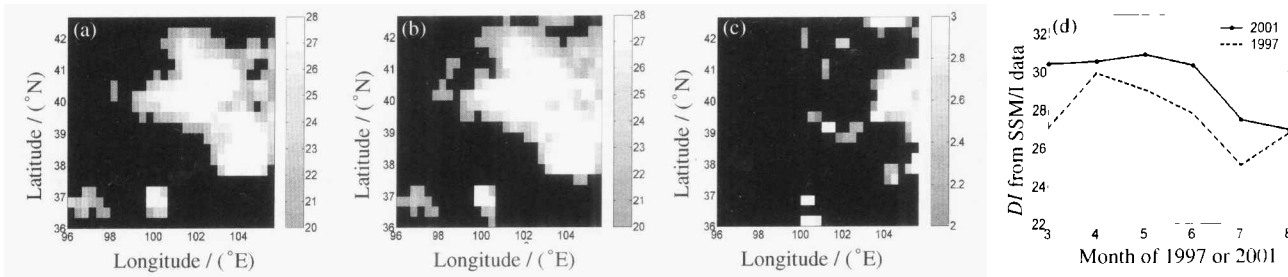


Fig. 5. Desertification index DI distribution. (a) Averaged DI distribution during March ~ August 1997, (b) averaged DI distribution during March ~ August 2001, (c) difference between (b) and (a), (d) DI variations at Yabulai.

3 Getis statistics of spatial auto-correlation

Statistics of spatial auto-correlation quantitatively evaluates the correlation of characteristic variable or parameter x over the whole region. In conventional statistics, all variables at different locations are always assumed as independent of each other. In environmental remote sensing, local radiative properties usually demonstrate highly spatial correlation, e. g. canopy growth or disappearance, drought or flooding in one location certainly affects the environment in another nearby location. The Getis statistics^[6-8] is studied for the range and clustering pattern of the variable x . Suppose there is a n -pixels image. Getis statistics expresses the sum of the weighted variable values within a specified distance d of a particular observation pixel i (including the i_{th} pixel) as a proportion of the sum of the variable values for the entire study area:

$$G_i^*(d) = \frac{\sum_{j=1}^n W_{ij}(d)x_j}{\sum_{j=1}^n x_j}, \quad (9)$$

where W_{ij} is a spatial weights matrix, and it is set to 1 as the pixel j is within distance d , otherwise it is equal to 0. The normalized Z -score is calculated as

$$Z_i(d) = \frac{[G_i^*(d) - E(G_i^*(d))]}{\sqrt{\text{Var}(G_i^*(d))}}. \quad (10)$$

Eq. (10) describes the clustering pattern of regional variable x . High positive Z values computed from Eq. (10) indicate clustering of high pixel val-

ues, while high negative ones denote clustering of low pixel values. With DI as a variable, we may examine the spatial correlation and clustering pattern of desertification. If a pixel has a correlation with a region identified as desert, the similarity in radiative properties between this pixel and the desert region reflects this kind of correlation, thus turning up a way to validate the extent of local desertification. With regard to this point, we cannot reach it by merely using of the above-mentioned difference of DI .

Fig. 6(a) and (b) present the distribution of normalized Z value using the Getis statistics for March ~ August 1997 and 2001, respectively. A merging tendency can be seen at the boundary of the two deserts in 2001. Meanwhile, the top-right corner of Fig. 6(c) shows a possible desertification happening to the northeast of Tengger Desert, where spatial correlation is identified.

The Getis statistics demonstrates spatial auto-correlation, and will not be affected by those variations in the whole region, e. g. increases of atmospheric temperature and opacity, etc. We can also find that some high DI values in Fig. 5(c) have disappeared in the Getis distribution of Fig. 6(c), which means a low correlation. The Getis statistics has great physical significance to see spatial variation of a whole region, and can provide a quantitative description for desertification information and its analysis.

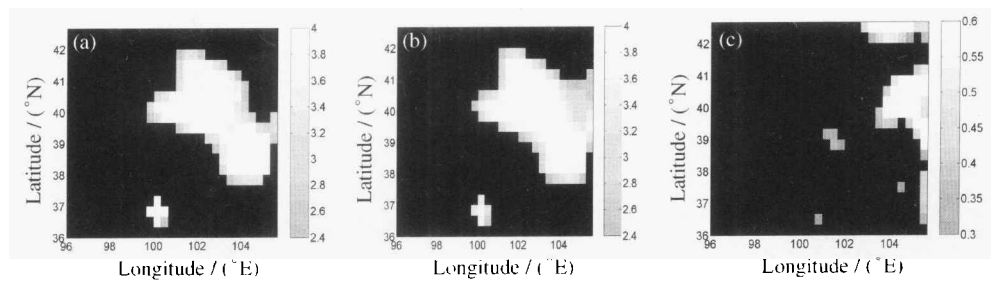


Fig. 6. Getis spatial correlation. (a) Getis distribution of DI in 1997, (b) Getis distribution of DI in 2001 and (c) Getis spatial correlation variations between 1997 and 2001.

4 Conclusions

In this paper, two SSM/I indexes, SDI and DI , are derived from the radiative transfer equation and are measured by multi-channel SSM/I observation. These indexes are applied to monitoring sandstorm occurrence and desertification. Significant increase of the SDI is identified during the sandstorm in Hunshandake Desert and its adjacent region in March 2002. It is also validated by China FY observation. Comparison of the variation of the DI index during March ~ August 1997 and 2001 shows boundary emergence and expansion of Badain Jaran Desert and Tengger Desert. The Getis statistics of the DI index is developed for quantitative description of spatial auto-correlation. It shows desertification variation and evolution. This study presents a theoretical approach and quantitative evaluation for monitoring sandstorm and desertification by satellite-borne microwave remote sensing.

References

- 1 Luo, J. Sandstorm surveillance wrap-up. The Remote Sensing Brief Report (in Chinese), 2002, (106 - 107): 1.
- 2 Chen, S. The Earth System Science (in Chinese). Beijing: China Science and Technology Press, 1998.
- 3 Jin, Y. Q. Analysis of SSM/I data over the desert of China. Chinese Journal of Remote Sensing (in Chinese), 1997, 1(3): 192.
- 4 Jin, Y. Q. Electromagnetic Scattering Modeling for Quantitative Remote Sensing. Singapore: World Scientific, 1994.
- 5 Goldhirsh, J. Attenuation and backscatter from a derived two-dimensional dust storm model. IEEE Trans. Antennas Propagat., 2001, 49(12): 1703.
- 6 Chen, Y. et al. Monitoring and evaluation of flooding extent by using the Getis statistics of the SSM/I. Proceedings of IGARSS, 1999, 14(3): 241.
- 7 Getis A. et al. The analysis of spatial association by use of distance statistics. Geographical Analysis, 1992, 24(3): 189.
- 8 Wulder, M. P. et al. Local spatial autocorrelation characteristics of remotely sensed imagery assessed with the Getis statistic. Int. J. Remote Sensing, 1998, 19(11): 2223.
- 9 Bhandari, S. M. Comments on monitoring of brightness temperature over India and adjoining regions using SSM/I data. Int. J. Remote Sensing, 2000, 21(16): 3187.